Use of $CuO/MgAl_2O_4$ and $La_{0.8}Sr_{0.2}FeO_3/\gamma\text{-}Al_2O_3$ in Chemical Looping Reforming System for Tar Removal from Gasification Gas

Martin Keller and Henrik Leion
Dept. of Chemical and Biological Engineering, Chalmers University of Technology, S-412 96 Göteborg, Sweden

Tobias Mattisson
Dept. of Energy and Environment, Chalmers University of Technology, S-412 96 Göteborg, Sweden

DOI 10.1002/aic.15034
Published online September 17, 2015 in Wiley Online Library (wileyonlinelibrary.com)

Biomass gasification gas contains condensable hydrocarbons usually referred to as "tars." The use of chemical-looping reforming (CLR) has been proposed as a downstream technology for tar removal. The tar removal capabilities and the regeneration properties of two particularly promising bed materials, $CuO/MgAl_2O_4$ and $La_{0.8}Sr_{0.2}FeO_3/\gamma\text{-}Al_2O_3$, were investigated using C_2H_4, C_6H_6, and C_7H_8 as tar surrogates. The material $La_{0.8}Sr_{0.2}FeO_3/\gamma\text{-}Al_2O_3$ exhibited high levels of conversion of all tar surrogates investigated, whereas $CuO/MgAl_2O_4$ showed less promising behavior. For this material, the C_2H_4 conversion in the absence of aromatic compounds was very high, but in the presence of monoaromatic compounds, the conversion of aromatics and C_2H_4 was poor. This indicates that monoaromatic compounds hinder the conversion of C_2H_4 effectively. Therefore, C_2H_4 may not always be a good choice as a tar surrogate and its suitability may depend on the mechanism of hydrocarbon conversion on the bed material surface in question. © 2015 American Institute of Chemical Engineers *AIChE J*, 62: 38–45, 2016
Keywords: biomass, chemical-looping reforming, gas cleaning, gasification, dual fluidized bed

Introduction and Background

Gasification of biomass presents a promising route to generate carbon-neutral synthesis gas ($CO + H_2$), which can then be further processed into valuable gaseous and liquid fuels such as substitute natural gas, dimethyl ether, or others.[1–3] In addition to the major syngas components, the raw gasification gas contains unwanted contaminants such as sulfur compounds, ammonia, and condensable hydrocarbons. The latter ones are often referred to as "tars"[4] and are particularly problematic due to their high condensation temperature which may give rise to fouling and blocking of downstream equipment.[5]

Hot catalytic tar removal has been proposed as a means of addressing this issue.[4,6] It can be achieved by either primary measures directly inside the gasifier, or by secondary measures downstream of the gasifier.[4,7] Secondary measures offer the advantage of greater flexibility in process parameters, such as operating temperature and additional steam injection, and a potentially higher degree of tar removal.[4,7] Such a catalytic cleaning step can be realized in various reactor configurations and a large number of different catalytic materials have been suggested and tested for their tar removal capability.[8] However, most catalysts tested suffer from deactivation primarily due to the formation of coke on the catalytically active surface.[9,10] Recently, a dual-fluidized bed reactor system has been proposed that circumvents this problem by continuously regenerating the catalyst in air in a similar way as it is conducted in a Fluid Catalytic Cracking unit.[11,12]

In this process, the bed material, active for tar removal, is circulated between a reformer, in which the bed material is contacted with the raw synthesis gas, and a regenerator, in which the bed material is regenerated by oxidizing coke deposits with air. When a metal oxide is utilized, which is able to transport some oxygen between these two reactors, the process is referred to as chemical-looping reforming of tars (in short CLR),[11] a process which is based on autothermal CLR for hydrogen production.[13] Figure 1 shows the proposed layout of such a system.

In the reformer of a CLR system, hydrocarbons contained in the raw gasification gas may be converted by numerous different reactions. These are either catalytic reactions on the surface of the bed material or noncatalytic reactions that modify the oxidation state of the bed material by oxygen transfer. In the regenerator, coke that has been deposited on the bed material surface can be oxidized with the oxygen supplied to the reactor and the bed material itself may also get reoxidized. The degree of oxidation of the bed material and, as a consequence, the degree of oxidation of the gasification gas may thus be controlled by the oxygen carrying capacity of the bed material, the recirculation rate of the bed material and/or by

Additional Supporting Information may be found in the online version of this article.

Correspondence concerning this article should be addressed to M. Keller at kellerm@chalmers.se.

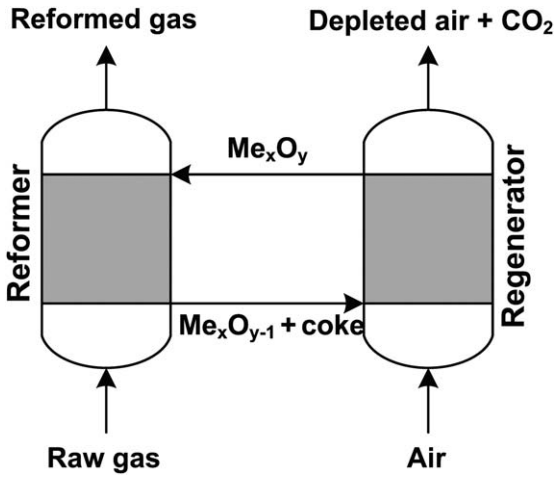

Figure 1. Schematic of the chemical looping reforming process for tar removal from biomass producer gas.

providing an under stoichiometric amount of oxygen to the regenerator. An overview of the numerous possible reaction pathways in the CLR system can be found elsewhere.[14]

Bed materials for CLR have been evaluated in a continuous unit at Chalmers University of Technology, namely the natural ore ilmenite,[11,15] synthetic Mn_3O_4 supported on ZrO_2[16] and NiO supported on α-Al_2O_3[15,17] with promising results. As the testing of bed materials in such a unit is laborious and does not allow for the detailed resolution of the reduction and oxidation properties of the materials, a small-scale, batch-wise fluidized bed reactor, where the bed material is exposed to reformer and regenerator conditions alternatingly, has been constructed.[14] In a previous study, this system was utilized to conduct a broad screening study of a variety of bed materials that may be of interest for the utilization in the CLR process. C_2H_4 was used as a tar surrogate, and it was found that the synthetic materials $CuO/MgAl_2O_4$ and $La_{0.8}Sr_{0.2}FeO_3/\gamma$-$Al_2O_3$ yielded high C_2H_4 conversion, while only low or moderate conversion of CH_4 was observed.

The aim of this study is thus to investigate the tar removal capabilities of these two promising materials using C_2H_4, C_6H_6, and C_7H_8 as tar surrogates. A methodology was established whereby the conversion of these surrogate compounds was determined as a function of time and thus in regions where the material transferred oxygen in addition to when the material was fully reduced and only catalytic reactions were occurring.

Experimental

Experimental setup

Experiments were conducted in a small-scale fluidized bed reactor made of quartz glass with an inner diameter of 22 mm immersed into an electric oven. An overview of the experimental setup is shown in Figure 2. Temperature and pressure drop over the fluidized bed were measured with a K-type thermocouple and pressure transducers, respectively. The gas was distributed via a porous plate on which 9 g of bed material were placed. Particles were of Geldart B type with bulk densities of around 1 g/mL. u_{mf} was about 0.01 m/s and u_0 was about 0.2 m/s. Bubbling fluidization of the bed was monitored and confirmed by differential pressure measurement over the bed. To emulate the circulation of the bed material between the regenerator and the reformer of a continuous CLR unit as described in Figure 1, the bed material was alternatingly exposed to reducing and oxidizing conditions. In between these exposures, the reactor was flushed with N_2 for 180 s. This change in inlet flow of gases was achieved with automatic magnetic valves as indicated in Figure 2. All the gases used were supplied by gas bottles and their flow rates were controlled by mass flow controllers. To emulate the reducing

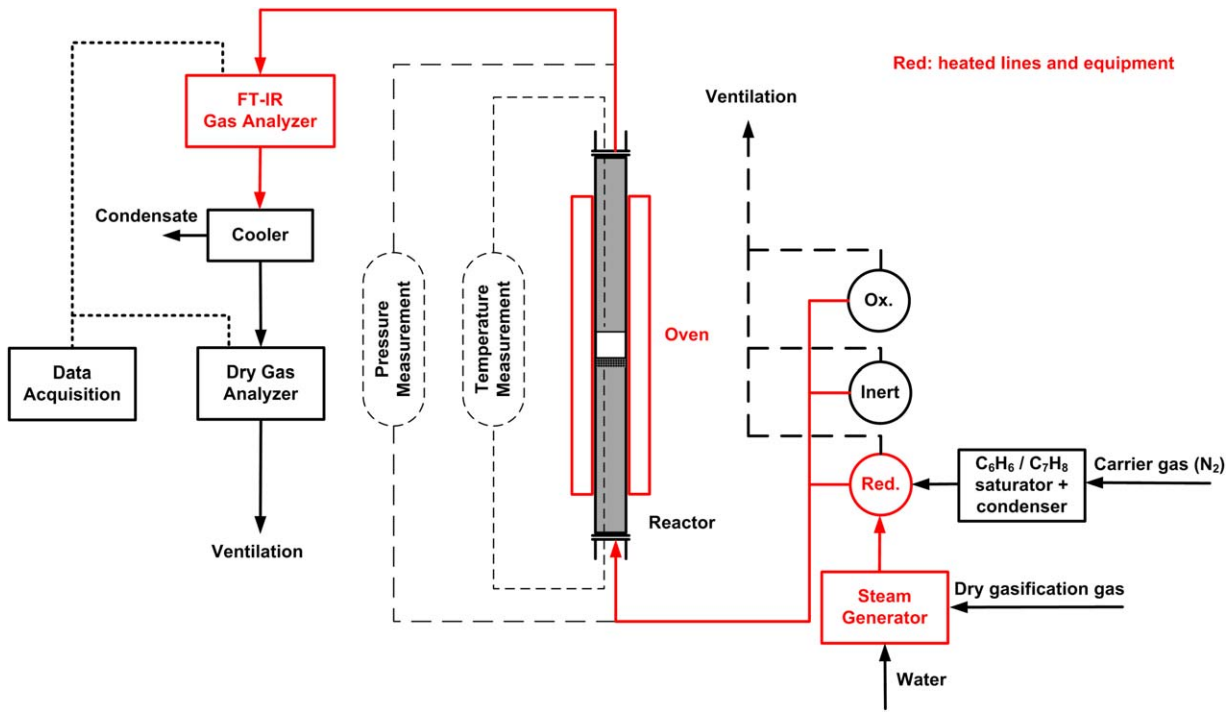

Figure 2. Schematic overview of the experimental setup.

[Color figure can be viewed in the online issue, which is available at wileyonlinelibrary.com.]

Table 1. Composition of Synthetic Gasification Gas Mixtures Used in the Experiments

Concentration in mol %	No Aromatics in Feed	C_6H_6 in Feed	C_7H_8 in Feed
N_2	50	48.6	48.6
H_2O	25	25	25
CO	10.75	10.75	10.75
CO_2	3.73	3.73	3.73
H_2	5.78	5.78	5.78
CH_4	3.5	3.5	3.5
C_2H_4	1.25	1.25	1.25
C_6H_6	–	1.4	–
C_7H_8	–	–	1.4

conditions in the reformer and to measure the gas conversion, the bed material was exposed to a synthetic gasification gas flow of 1 L_N/min for 1000 s. Most experiments were conducted with three different gas mixtures as outlined in Table 1. All mixtures contained C_2H_4, with or without aromatics. Additionally, one series of experiments with $CuO/MgAl_2O_4$ was performed in which the C_6H_6 concentration was varied between 0 and 1.4 mol % and the N_2 concentration between 50 and 48.6 mol %, while keeping the concentrations of all other gases constant.

The addition of aromatics to the N_2 carrier gas stream was achieved by saturating the gas with C_6H_6 or C_7H_8 at room temperature and then cooling the gas down to the desired temperature in a laboratory cooler with countercurrent flow of cooling fluid. That way, the aromatics concentration in the N_2 carrier gas stream corresponds to the saturation concentration of the aromatic compound at the temperature of the cooling fluid. This mixture is then mixed with the steam/gasification gas mixture, as seen in Figure 2. After the exposure of the bed material to the reducing gas, the reactor was flushed with N_2 and then the bed material was exposed to a flow of 0.6 L_N/min of synthetic air (consisting of 20.9% O_2 in N_2) for 360–480 s to emulate the oxidizing conditions in the regenerator and to achieve full reoxidation of the bed material. The system was operated at atmospheric pressure and the temperature was varied between 750, 800, and 850°C for each of the bed materials investigated. Experiments were repeated three times to ensure reproducibility. Unless indicated otherwise, the data presented here are averages of the three experiments. The standard error in the degree of hydrocarbon conversion from these three cycles was about 0.5–2% absolute.

Gas analysis

The wet effluent gas was transported in heated lines to a Thermo-Scientific iS50 FTIR analyzer equipped with a heated gas cell. The FTIR analyzer was carefully calibrated for the quantification of the concentration of CO, CO_2, H_2O, CH_4, C_2H_4, C_2H_6, C_6H_6, and C_7H_8 by conducting calibration experiments with both pure gases diluted in N_2 and various wet and dry gas mixtures. In total, over 200 calibration compositions were generated and evaluated to obtain accurate measurements. Gas concentrations were measured every 4 s with the FTIR. After the gas was cooled and the condensate removed from the gas stream, the dry effluent gas was then sent to a dry gas analyzer to determine the concentration of H_2 and O_2 with a thermal conductivity and a paramagnetic gas sensor.

Bed materials

Experiments were conducted with either 9 g of $CuO/MgAl_2O_4$ or $La_{0.8}Sr_{0.2}FeO_3/\gamma$-$Al_2O_3$ sieved to a size range of 125–180 μm. Additionally, empty reactor experiments were conducted to determine the extent of homogeneous gas-phase reactions, which could not be attributed to the bed material. To determine the effect of the impregnation of $La_{0.8}Sr_{0.2}FeO_3$/on γ-Al_2O_3 one experiment was also conducted with 9 g of unimpregnated Puralox NWa155 γ-Al_2O_3 calcined analogously before the experiment at 1100°C for 2 h. The composition, production parameters, and BET surface area of the synthetic particles are summarized in Table 2. The $CuO/MgAl_2O_4$ particles were spray dried from fine powders, whereas the $La_{0.8}Sr_{0.2}FeO_3/\gamma$-$Al_2O_3$ particles were manufactured by impregnation. Here, a fine powder of $La_{0.8}Sr_{0.2}FeO_3$, which was obtained by solid-state synthesis route and ball milling, was suspended in a slurry containing large γ-Al_2O_3 particles to which the perovskite primary particles attached. The considerably larger surface area of the $La_{0.8}Sr_{0.2}FeO_3/\gamma$-$Al_2O_3$ particles can be explained by the higher surface area of its original support material (Puralox NWa155, 145 m^2/g) in comparison to the surface area of the support material of the $CuO/MgAl_2O_4$ particles (Baikowski S30CR, 30 m^2/g).

Characterization of bed materials

The BET surface area of the bed materials was determined by N_2 adsorption (Micromeritics, TriStar 3000) before and after the experiments. The major crystalline phases of the bed materials were identified before and after the experiments using powder x-ray diffraction (Bruker D8 advance) with CuKα radiation.

Data evaluation

The conversion of the various hydrocarbons C_xH_y, $\gamma_{C_xH_y}$, is calculated from a molar balance of the inlet C_xH_y and the outflowing C_xH_y as determined by FTIR measurement

$$\gamma_{C_xH_y} = \frac{x_{C_xH_y,\,in}\,\dot{n}_{in} - x_{C_xH_y,\,out}\,\dot{n}_{out}}{x_{C_xH_y,\,in}\,\dot{n}_{in}} \times 100\% \qquad (1)$$

The coke formation on the bed material is calculated as percentage of the total C fed during the exposure to the gasification gas by integrating the CO and CO_2 profiles during reoxidation of the bed material

$$\text{Coke formation} = \frac{\int_{t_{reoxidation,\,start}}^{t_{reoxidation,\,end}} \left(x_{CO,out} + x_{CO_2,out}\right) \dot{n}_{out}\, dt}{\int_{t_{reduction,\,start}}^{t_{reduction,\,end}} \left(x_{CO,in} + x_{CO_2,in} + x_{CH_4,in} + 2x_{C_2H_4,in} + 6x_{C_6H_6,in} + 7x_{C_7H_8,in}\right) \dot{n}_{in}\, dt} \times 100\% \qquad (2)$$

The degree of gas oxidation φ, which describes to which degree the synthetic gasification gas is oxidized by oxygen supplied by the bed material, is calculated from the oxygen required for full oxidation of the gas

$$\varphi = 1 - \frac{\left(\frac{1}{2}x_{CO,out} + \frac{1}{2}x_{H_2,out} + 2x_{CH_4,out} + 3x_{C_2H_4,out} + 7.5x_{C_6H_6,out} + 9x_{C_7H_8,out}\right) \times \dot{n}_{out}}{\left(\frac{1}{2}x_{CO,in} + \frac{1}{2}x_{H_2,in} + 2x_{CH_4,in} + 3x_{C_2H_4,in} + 7.5x_{C_6H_6,in} + 9x_{C_7H_8,in}\right) \times \dot{n}_{in}} \quad (3)$$

Results

In Figure 3, the recorded gas concentration profiles are shown for an experiment with $CuO/MgAl_2O_4$ as a bed material and C_6H_6 in the gasification gas at $T = 800°C$. First, the fully oxidized bed material is exposed to the gasification gas and gets reduced to its thermodynamically stable form under the experimental conditions. This results in high H_2O and CO_2 concentrations. After the material has been equilibrated and does not provide oxygen to the gas any longer, the composition of the flue gas stabilizes. Afterward, the reactor is first flushed with N_2 and then synthetic air is introduced to the reactor, resulting in an oxidation of possible coke deposits and a reoxidation of the bed material. In this experiment, the peak of the CO_2 concentration resulting from the combustion of the coke is rather small, this indicates that quite a small amount of coke has been formed. During all experiments, no other hydrocarbons than the ones shown in Figure 3 were detected, with the exception that minor quantities of C_2H_2 were detected in the empty reactor experiments.

Upon initial exposure of the bed material to the gasification gas, there is an oxygen transfer from the bed material to the gas phase. Thus, initially, the gasification gas is primarily oxidized to CO_2 and H_2O which is followed by a brief period of partial oxidation of the gas, see Figure 3.

Figure 4 shows the conversion of hydrocarbons with either C_6H_6 in the feed, C_7H_8 in the feed, or with no aromatics in the feed for the two bed materials as a function of the degree of gasification gas oxidation at $T = 800°C$. Here, $\varphi = 1$ corresponds to complete combustion, while at $\varphi = 0$ there would be no oxygen transferred to the gas.

When C_6H_6 or C_7H_8 is fed to the reactor with the Cu-based material, the catalytic activity at low φ is poor, as is evident in Figures 4a, b. When feeding C_6H_6, however, the addition of only a small fraction of oxygen results in a significant increase in the C_2H_4 conversion. It is also evident that C_2H_4 is preferentially oxidized over C_6H_6, which is preferentially oxidized over CH_4 which is even generated during partial oxidation of the gasification gas (a negative conversion value indicating a generation of that compound). For the C_7H_8 experiments, somewhat more oxygen is needed to achieve a similar effect.

From Figures 4c, d, it can be seen that over $La_{0.8}Sr_{0.2}FeO_3/\gamma\text{-}Al_2O_3$, due to the high degree of aromatics conversion, it is difficult to observe preferential oxidation of C_2H_4 over either C_6H_6 or C_7H_8.

Table 2. Composition, Production Parameters, and Surface Area of Bed Materials

	$CuO/MgAl_2O_4$	$La_{0.8}Sr_{0.2}FeO_3/\gamma\text{-}Al_2O_3$
Composition	40 wt % CuO, 60 wt % $MgAl_2O_4$ (Baikowski S30CR)	10 wt %. $La_{0.8}Sr_{0.2}FeO_3$, 90 wt % $\gamma\text{-}Al_2O_3$ (Puralox NWa155)
Production parameters	Spray drying, calcined for 4 h @ 1030°C	Impregnation, calcined for 2 h @ 1100°C
BET surface area (m^2/g)	7.85	47.03

At the other two investigated temperatures of $T = 750°C$ and $T = 850°C$, qualitatively similar trends could be observed that are shown in Supporting Information Figures S1 and S2.

XRD analysis of the oxidized, fresh bed materials, and the bed materials retrieved after exposure to the gasification gas without reoxidation revealed that CuO is fully reduced to Cu during exposure, whereas the $La_{0.8}Sr_{0.2}FeO_3$ was found to be stable during exposure. Accordingly, $CuO/MgAl_2O_4$ transported about 8 wt % of its mass as oxygen from the oxidation period to the reduction period. $La_{0.8}Sr_{0.2}FeO_3/\gamma\text{-}Al_2O_3$, however, transported only 0.45 wt % of its mass as oxygen.

In Figures 5a, b, the catalytic conversion levels of C_6H_6 and C_7H_8 are shown as a function of reactor temperature for both materials investigated and the empty reactor. Figure 5c shows the degree of C_6H_6 generation from the dealkylation of C_7H_8. The values presented in Figures 5, 6, 8, and 9 are averaged values of all three repetitions of the experiment where data are taken during the stable period from 500 to 1000 s (see Figure 3) in which no oxygen is transferred from the particles to the gas phase any longer. It can be observed that the $La_{0.8}Sr_{0.2}FeO_3/\gamma\text{-}Al_2O_3$ achieves rather high conversion levels of both C_6H_6 and C_7H_8, whereas the conversion of aromatics by the $CuO/MgAl_2O_4$ is poor and only slightly higher than the conversion observed in an empty reactor. Generally, conversion levels increase with temperature. The benzene conversion is generally lower than the toluene conversion, likely due to the dealkylation of C_7H_8 to C_6H_6.

In Figure 6, the conversion of C_2H_4 in the absence of aromatics, in the presence of C_6H_6, and in the presence of C_7H_8 over different bed materials and as a function of reactor temperature is shown. It can be observed that for the empty reactor and $La_{0.8}Sr_{0.2}FeO_3/\gamma\text{-}Al_2O_3$ experiments, the presence of aromatics results only in a rather small decrease of C_2H_4 conversion. Over $CuO/MgAl_2O_4$, the presence of aromatics in the

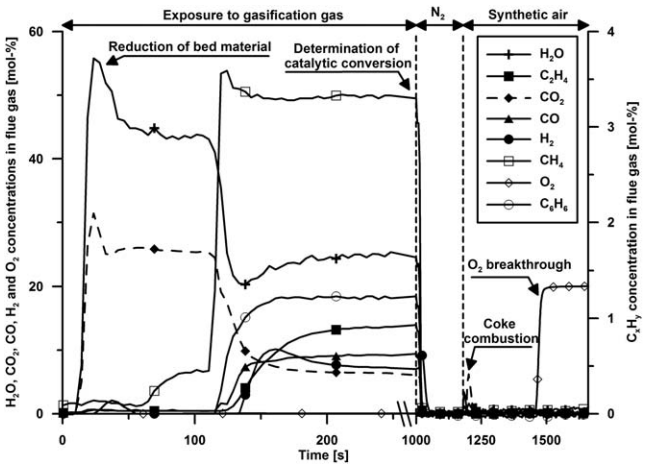

Figure 3. Recorded gas concentration profile during exposure to gasification gas with C_6H_6 in feed and subsequent reoxidation in air of $CuO/MgAl_2O_4$ at a temperature of $T = 800°C$ (note that the *x* axis is broken after the gas concentrations stabilize after 250 s).

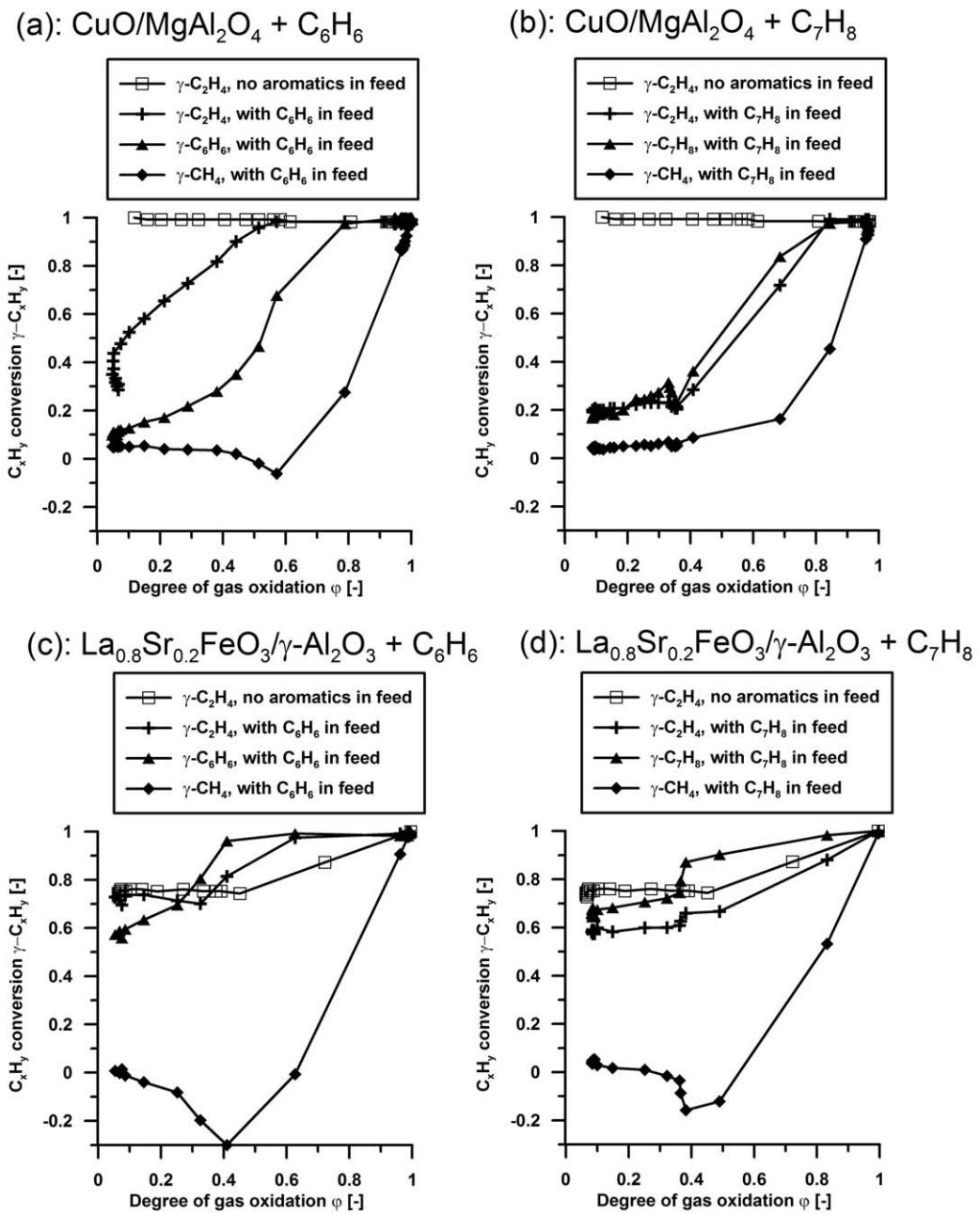

Figure 4. Hydrocarbon conversion as a function of degree of gas oxidation at $T = 800°C$ over (a), (b) $CuO/MgAl_2O_4$ and (c), (d) $La_{0.8}Sr_{0.2}FeO_3/\gamma\text{-}Al_2O_3$ with (a), (c) C_6H_6 in the feed and (b), (d) C_7H_8 in the feed (right).

The case where no aromatics are fed is also included. The negative conversion values for methane indicate formation of CH_4.

gasification gas causes a drastic decrease in C_2H_4 conversion, resulting in conversion levels that are only marginally higher than those observed in an empty reactor.

Additionally, the amount of coke formed on the bed materials during their exposure to the gasification gas was determined. For the empty reactor and $La_{0.8}Sr_{0.2}FeO_3/\gamma\text{-}Al_2O_3$, coke formation was minimal and the resulting CO_2 concentration peaks during reoxidation were hardly quantifiable with the current measurement setup. The coke formation on $CuO/MgAl_2O_4$ calculated as mol % of total carbon fed to the reactor during one reduction period is shown as function of temperature in Figure 7. It can be seen that on $CuO/MgAl_2O_4$ significant quantities of coke of up to 5% of the total carbon fed were formed when the material was exposed to the gasification gas and reduced to Cu in the absence of aromatics. However, as soon as aromatics were present in the gas, the formation of coke was drastically suppressed, as can be seen in Figure 7.

To evaluate the magnitude of the effect of the presence of aromatics on the C_2H_4 conversion over $CuO/MgAl_2O_4$, experiments were conducted with a varying concentration of C_6H_6 in the syngas at 800°C. The conversion of C_6H_6 and C_2H_4 as a function of the C_6H_6 concentration in the feed is shown in Figure 8. In these experiments, the C_6H_6 conversion was found to be very low at all C_6H_6 feed concentrations. The inhibiting effect of C_6H_6 on the C_2H_4 conversion was found to decrease with decreasing C_6H_6 concentration; however, not in a linear fashion. From 1.4 mol % down to 0.6 mol % C_6H_6, C_2H_4 conversion remains almost constant at a low level. At lower concentrations of C_6H_6, the inhibiting effect of C_6H_6 on

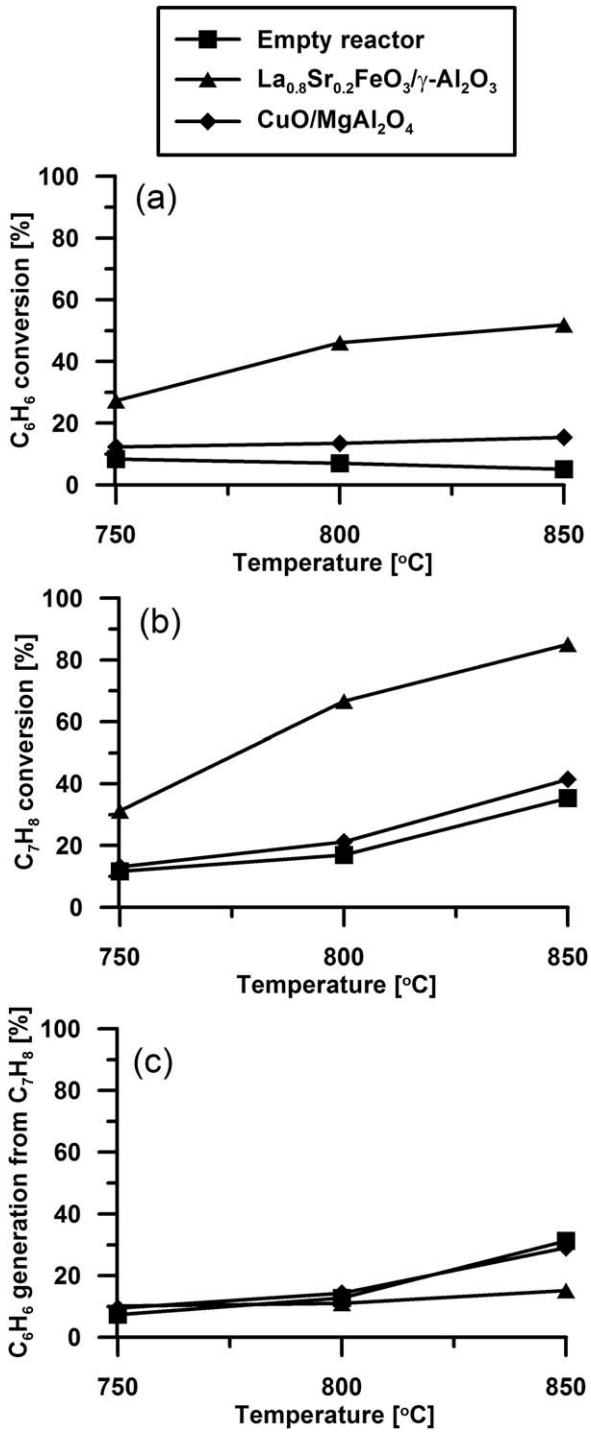

Figure 5. Conversion of (a) C_6H_6, (b) C_7H_8, and (c) generation of C_6H_6 from C_7H_8 over different bed materials and as a function of reactor temperature.

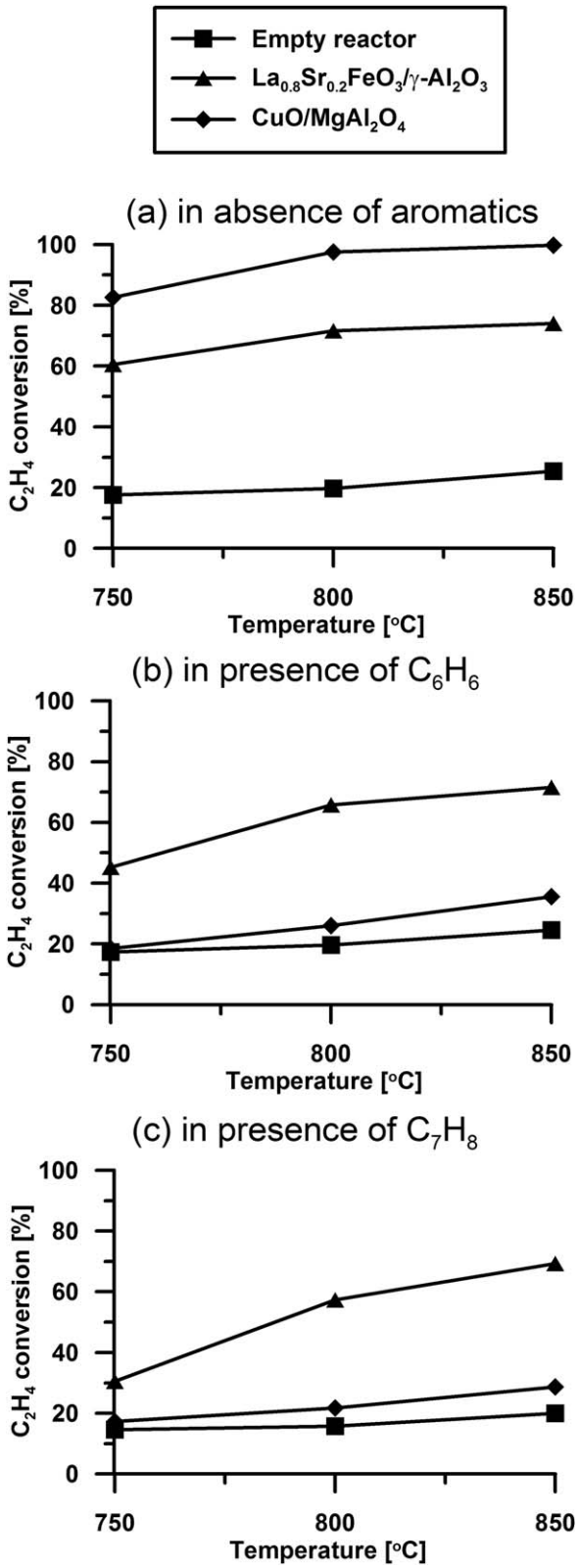

Figure 6. Conversion of C_2H_4 (a) in the absence of aromatics, (b) in the presence of 1.4 mol % C_6H_6 in the feed, and (c) in the presence of 1.4 mol % C_7H_8 in the feed over different bed materials and as a function of reactor temperature.

C_2H_4 conversion decreases significantly and C_2H_4 conversion increases accordingly.

To differentiate between the effect of $La_{0.8}Sr_{0.2}FeO_3$ and the mesoporous γ-Al_2O_3 support on the performance of the $La_{0.8}Sr_{0.2}FeO_3/\gamma$-$Al_2O_3$ bed material for tar reforming, experiments were also conducted with nonimpregnated, pure γ-Al_2O_3. In Figure 9, the conversion of C_2H_4 and C_6H_6 over $La_{0.8}Sr_{0.2}$-FeO_3/γ-Al_2O_3 and γ-Al_2O_3 as a function of reactor temperature is displayed. The conversion of C_2H_4 is significantly improved by the impregnation with $La_{0.8}Sr_{0.2}FeO_3$. C_6H_6 conversion over γ-Al_2O_3 was found to be very low, and only marginally higher than the conversion in an empty reactor.

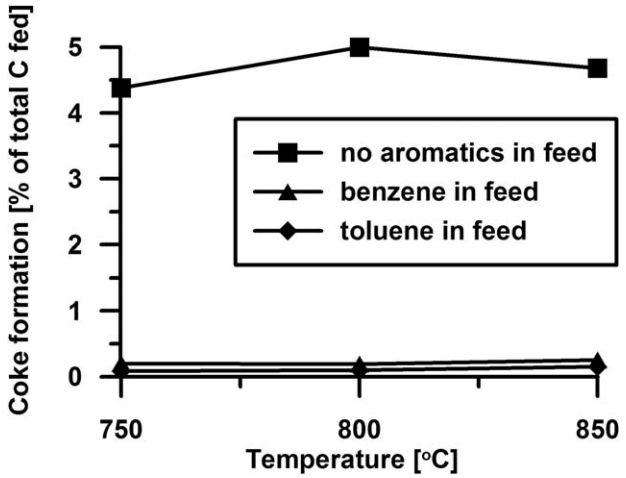

Figure 7. Coke formation on $CuO/MgAl_2O_4$ as a function of reactor temperature.

Discussion

In this study, two synthetic bed materials, $CuO/MgAl_2O_4$ and $La_{0.8}Sr_{0.2}FeO_3/\gamma\text{-}Al_2O_3$ were investigated for their ability to remove the tar surrogates C_2H_4, C_6H_6, and C_7H_8 from biomass gasification gas using chemical-looping tar reforming. It was found that for $La_{0.8}Sr_{0.2}FeO_3/\gamma\text{-}Al_2O_3$ the conversion levels of C_6H_6 and C_7H_8 are rather high, albeit lower than the conversion of C_2H_4. It was found that the $La_{0.8}Sr_{0.2}FeO_3$ phase is active for the C_6H_6 conversion, as the tar reforming performance of the nonimpregnated $\gamma\text{-}Al_2O_3$, calcined under the same conditions, was poor. This is line with previous research[18] where it was observed that mesoporous $\gamma\text{-}Al_2O_3$ is highly effective for the removal of heavy tar. The heavy tar is deposited as coke on the $\gamma\text{-}Al_2O_3$ and the preformed coke is then active for the decomposition of polyaromatic compounds.[18] In our experiments, heavy tars were absent and such a pathway of tar decomposition is thus unlikely.

In general, the degree of conversion of all tar species increases as a function of temperature, which indicates that, for $La_{0.8}Sr_{0.2}FeO_3/\gamma\text{-}Al_2O_3$, the use of C_2H_4 as a tar surrogate may serve as a good indicator for the general behavior of monoaromatic tar compounds. However, it was found that the same does not hold true

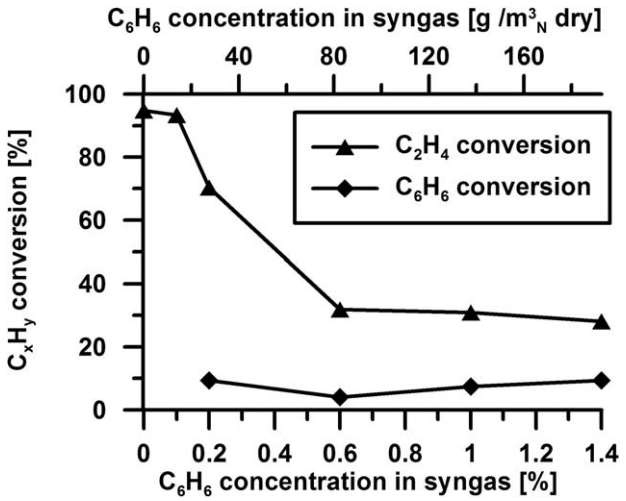

Figure 8. Conversion of C_6H_6 and C_2H_4 over $CuO/MgAl_2O_4$ as a function of the C_6H_6 concentration in the feed stream at $T = 800°C$.

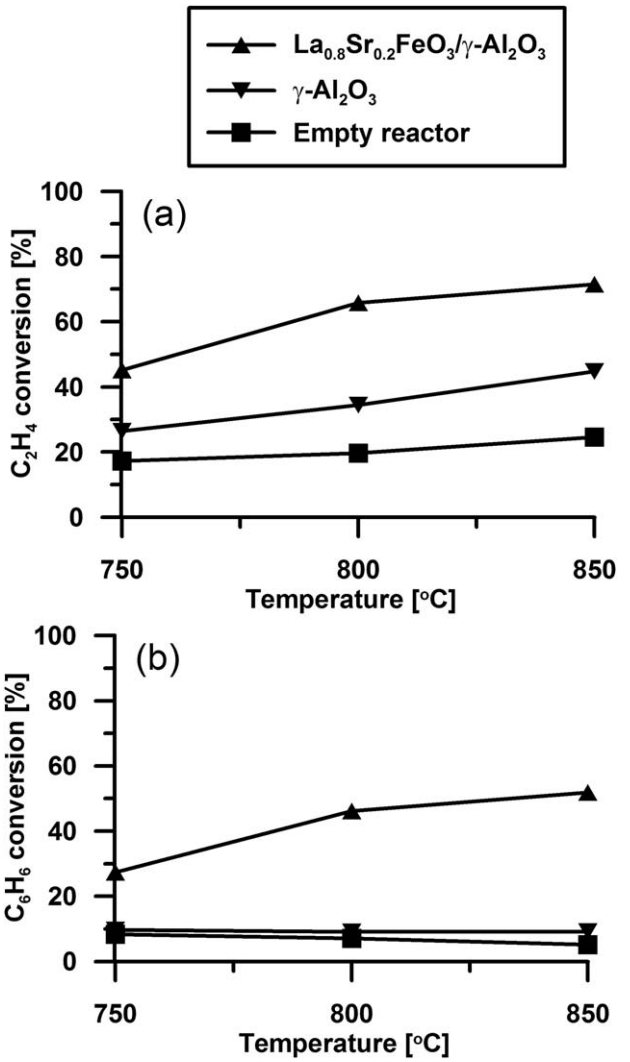

Figure 9. Conversion of (a) C_2H_4 and (b) C_6H_6 over $La_{0.8}Sr_{0.2}FeO_3/\gamma\text{-}Al_2O_3$ and $\gamma\text{-}Al_2O_3$ as a function of reactor temperature.

for the conversion over $CuO/MgAl_2O_4$. For this material, the C_2H_4 conversion in the absence of aromatics was found to be very high, approaching 98% at 800°C. However, the conversion of the monoaromatic compounds such as C_6H_6 was low, less than 14% at the same temperature, and C_2H_4 as a tar surrogate is therefore not indicative for the conversion of monoaromatic compounds. Furthermore, the presence of aromatics inhibited the conversion of C_2H_4 drastically. The extent of this inhibition was found to depend on the partial pressure of C_6H_6 in the feed gas. This inhibition, which is only observed for the Cu-based material, could be caused by different mechanisms of hydrocarbon conversion over the two investigated materials. It was observed that $La_{0.8}Sr_{0.2}FeO_3/\gamma\text{-}Al_2O_3$ converted C_2H_4 and aromatics to syngas to a large extent, but over $CuO/MgAl_2O_4$, in the absence of aromatics, the C_2H_4 is instead forming significant quantities of coke. This coke formation is not observed with monoaromatic compounds and even suppressed by their existence.

From the data obtained in this study, the mechanism of this suppression can only be speculated. In previous research it was observed that, under similar experimental conditions, carbon is deposited on copper surfaces from mixtures of steam, H_2, and alkenes in the form of layered coke.[19] When comparing the adsorption energy on a Cu(111) surface of C_2H_4

($\sim$0.13 eV)[20] with that of C_6H_6 ($\sim$0.6 eV)[21] one may assume that, in the presence of both C_6H_6 and C_2H_4, C_6H_6 adsorbs preferentially on the Cu surface and may form a monolayer or even graphene under the experimental conditions of this study. Cu is well known to be a potent catalyst for the formation of graphene.[22] Due to the presence of steam in the gas and therefore a rather high oxygen potential of the gas, the formation of graphene oxide may even be plausible.[23] In any case, such a layer may then block the copper surface for the adsorption of C_2H_4 and thus inhibit the formation of coke from C_2H_4. The observation that C_2H_4 conversion decreases sharply with increasing C_6H_6 concentration in the feed further corroborates the existence of an inhibitory effect of monoaromatics on the coke formation from C_2H_4 on the Cu surface.

Conclusions

Two promising synthetic bed materials, $CuO/MgAl_2O_4$ and $La_{0.8}Sr_{0.2}FeO_3/\gamma$-$Al_2O_3$ were investigated in a small-scale fluidized bed for their ability to remove the tar surrogates C_2H_4, C_6H_6, and C_7H_8 from gasification gas. It was observed that $La_{0.8}Sr_{0.2}FeO_3/\gamma$-$Al_2O_3$ exhibited high levels of conversion of all tar surrogates investigated. A different picture was obtained for the $CuO/MgAl_2O_4$ material. Here, C_2H_4 conversion in the absence of aromatic compounds was very high, but in the presence of monoaromatic compounds, the conversion of aromatics and C_2H_4 was poor. At $T = 800$°C, the conversion of C_2H_4 dropped from 97 to 26% in the presence of C_6H_6. This indicates that the presence of aromatic compounds hinders the conversion of C_2H_4 considerably.

Thus, the use of C_2H_4 as an indicator for the conversion of aromatic compounds may not always be wise and its suitability may depend on the mechanism of hydrocarbon conversion on the active surface of the bed material in question.

Acknowledgments

This work has been supported by the Swedish Gasification Center and the Chalmers Energy Area of Advance. The $La_{0.8}Sr_{0.2}FeO_3/\gamma$-$Al_2O_3$ investigated in this work was produced and kindly provided by SINTEF, Trondheim, Norway.

Notation

γ = conversion of hydrocarbon
φ = degree of gas oxidation
$\dot{n}$ = molar flow rate, mol s^{-1}
x = molar fraction

Subscripts

in = gas flowing into the experimental reactor
out = gas flowing out from the experimental reactor

Abbreviations

BET = Brunauer–Emmett–Teller
CLC = chemical looping combustion
CLR = chemical looping reforming
FTIR = Fourier transform infrared
XRD = x-ray diffraction

Literature Cited

1. Bridgwater A. Renewable fuels and chemicals by thermal processing of biomass. *Chem Eng J*. 2003;91(2–3):87–102.
2. Demirbas A. Progress and recent trends in biofuels. *Prog Energy Combust Sci*. 2007;33(1):1–18.
3. Tock L, Gassner M, Maréchal F. Thermochemical production of liquid fuels from biomass: thermo-economic modeling, process design and process integration analysis. *Biomass Bioenergy*. 2010;34(12):1838–1854.
4. Torres W, Pansare SS, Goodwin JG. Hot gas removal of tars, ammonia, and hydrogen sulfide from biomass gasification gas. *Catal Rev*. 2007;49(4):407–456.
5. Li C, Suzuki K. Tar property, analysis, reforming mechanism and model for biomass gasification—an overview. *Renew Sustain Energy Rev*. 2009;13(3):594–604.
6. Abu El-Rub Z, Bramer EA, Brem G. Review of catalysts for tar elimination in biomass gasification processes. *Ind Eng Chem Res*. 2004;43(22):6911–6919.
7. Devi L, Ptasinski KJ, Janssen FJJG. A review of the primary measures for tar elimination in biomass gasification processes. *Biomass Bioenergy*. 2002;24:125–140.
8. Shen Y, Yoshikawa K. Recent progresses in catalytic tar elimination during biomass gasification or pyrolysis—a review. *Renew Sustain Energy Rev*. 2013;21:371–392.
9. Corella J, Aznar MP, Delgado J, Martinez MP, Aragües JL. The deactivation of tar cracking stones (dolomites, calcites, magnesites) and of commercial methane steam reforming catalysts in the upgrading of the exit gas from steam fluidized bed gasifiers of biomass and organic wastes. *Stud Surf Sci Catal*. 1991;68:249–252.
10. Bain RL, Dayton DC, Carpenter DL, Czernik SR, Feik CJ, French RJ, Magrini-Bair KA, Phillips SD. Evaluation of catalyst deactivation during catalytic steam reforming of biomass-derived syngas. *Ind Eng Chem Res*. 2005;44(21):7945–7956.
11. Lind F, Seemann M, Thunman H. Continuous catalytic tar reforming of biomass derived raw gas with simultaneous catalyst regeneration. *Ind Eng Chem Res*. 2011;50(20):11553–11562.
12. Dayton D, Kataria A, Gupta R. Biomass gas cleanup using a therminator. 2012. http://www.osti.gov/scitech/biblio/1035816. DOI: 10.2172/1035816.
13. Ryden M, Lyngfelt a, Mattisson T. Synthesis gas generation by chemical-looping reforming in a continuously operating laboratory reactor. *Fuel*. 2006;85(12–13):1631–1641.
14. Keller M, Leion H, Mattisson T, Thunman H. Investigation of natural and synthetic bed materials for their utilization in chemical looping reforming for tar elimination in biomass-derived gasification gas. *Energy Fuels*. 2014;28:3833–3840.
15. Lind F, Berguerand N, Seemann M, Thunman H. Ilmenite and nickel as catalysts for upgrading of raw gas derived from biomass gasification. *Energy Fuels*. 2013;27:997–1007.
16. Lind F, Israelsson M, Seemann M, Thunman H. Manganese oxide as catalyst for tar cleaning of biomass-derived gas. *Biomass Convers Biorefinery*. 2012;2(2):133–140.
17. Berguerand N, Lind F, Israelsson M, Seemann M, Biollaz S, Thunman H. Use of nickel oxide as a catalyst for tar elimination in a chemical-looping reforming reactor operated with biomass producer gas. *Ind Eng Chem Res*. 2012;51(51):16610–16616.
18. Hosokai S, Hayashi J-I, Shimada T, Kobayashi Y, Kuramoto K, Li C-Z, Chiba T. Spontaneous generation of tar decomposition promoter in a biomass steam reformer. *Chem Eng Res Des*. 2005;83(9):1093–1102.
19. Jackson PRS, Young DJ, Trimm DL. Coke deposition on and removal from metals and heat-resistant alloys under steam-cracking conditions. *J Mater Sci*. 1986;21:4376–4384.
20. Skibbe O, Vogel D, Binder M, Pucci A, Kravchuk T, Vattuone L, Venugopal V, Kokalj A, Rocca M. Ethene stabilization on Cu(111) by surface roughness. *J Chem Phys*. 2009;131(2):024701.
21. Choi J-H, Li Z, Cui P, Fan X, Zhang H, Zeng C, Zhang Z. Drastic reduction in the growth temperature of graphene on copper via enhanced London dispersion force. *Sci Rep*. 2013;3:1925.
22. Li X, Cai W, An J, Kim S, Nah J, Yang D, Piner R, Velamakanni A, Jung I, Tutuc E, Banerjee SK, Colombo L, Ruoff RS. Large-area synthesis of high-quality and uniform graphene films on copper foils. *Science*. 2009;324(5932):1312–1314.
23. Chu JH, Kwak J, Kim S-D, Lee MJ, Kim JJ, Park S-D, Choi J-K, Ryu GH, Park K, Kim SY, Kim JH, Lee Z, Kim Y-W, Kwon S-Y. Monolithic graphene oxide sheets with controllable composition. *Nat Commun*. 2014;5:3383.

Manuscript received May 14, 2015, and revision received Aug. 20, 2015.